Cellulose (2023) 30:801–813
https://doi.org/10.1007/s10570-022-04967-y

ORIGINAL RESEARCH

Cellulose dissolution and conversion into 5-hydroxymethylfurfural in mixed molten salt hydrate

Chunjie Wei · Gang Liu · Yujiao Xie · Zhongyuan Sun · Chang Liu · Feng Song · Hongyou Cui

Received: 22 July 2022 / Accepted: 22 November 2022 / Published online: 1 December 2022

Abstract Molten salt hydrate (MSH) is a good solvent for cellulose dissolution and an effective catalyst for cellulose conversion. In this work, a series of MSH was evaluated in terms of cellulose dissolvability, regeneration performance, and catalytic activity in cellulose conversion into 5-hydroxymethylfurfural (HMF). $ZnBr_2{\cdot}3H_2O$–$LiCl{\cdot}3H_2O$ showed good performance on cellulose dissolution and conversion. The effects of $ZnBr_2{\cdot}3H_2O$ concentration, reaction temperature, and time on cellulose conversion into HMF in $ZnBr_2{\cdot}3H_2O$–$LiCl{\cdot}3H_2O$ were optimized, and 48.7% HMF yield was reached at 60 wt.% $ZnBr_2{\cdot}3H_2O$. The species of $ZnBr_2{\cdot}3H_2O$–$LiCl{\cdot}3H_2O$ were analyzed, and the function of species concentration was correlated with the product yield from the conversion of fructose. It was found that Br^- and H^+ were the active species for fructose dehydration into HMF. $ZnBr_3^-$ and H^+ catalyzed the conversion of fructose into furfural, which competed with the production of HMF. The reaction mechanism was proposed to understand the cooperate of species in MSH for cellulose conversion.

Keywords Cellulose dissolution · Conversion · 5-Hydroxymethylfurfural · Molten salt hydrate

Introduction

The development and utilization of biomass-based renewable energy sources have been paid attention with increasing concerns to environmental and energy issues (Ashokkumar et al. 2021; Cho et al. 2020). Cellulose, a high molecular weight homopolymer formed by glucose units connected through β-(1–4) glycosidic linkages, is regarded as one of the most important biomass materials due to the advantages of rich reserves, wide sources, safety, nontoxicity, and biodegradability (Ab Rasid et al. 2021). The dissolution of cellulose plays an important role in its conversion to produce glucose and other platform compounds, and then further produce energy, fuel, and valuable chemicals (Feng and Chen 2008). The dissolvability of cellulose is poor in water and many organic solvents. Therefore, finding a cellulose solvent with good dissolvability and high efficiency is necessary.

Supplementary Information The online version contains supplementary material available at https://doi.org/10.1007/s10570-022-04967-y.

C. Wei · G. Liu · Y. Xie (✉) · Z. Sun · F. Song · H. Cui (✉)
School of Chemistry and Chemical Engineering, Shandong University of Technology, Zibo 255000, China
e-mail: yujiaoxie@sdut.edu.cn

H. Cui
e-mail: cuihy@sdut.edu.cn

C. Liu
College of Chemical Engineering, State Key Laboratory of Materials-Oriented Chemical Engineering, Nanjing Tech University, Nanjing 211816, China

Molten salt hydrate (MSH) is a highly concentrated aqueous solution of inorganic salts with a molar water-to-salt ratio close to the coordination number of the strongest hydrated cations, and has the advantages of easy preparation, low cost, and environmental friendliness (Emons 1988). In MSH, the inorganic salt is hydrolyzed in water and produces complex ion forms. The interaction between cations and water molecules in the coordination sphere leads to a decrease in the charge density of the surrounding hydrogen atoms and the formation of positively charged protons–Brønsted acid (Rodriguez Quiroz et al. 2019a). Cations form Lewis acidic centers with hydroxyl ions and anions.

The dissolution of cellulose in MSH is gaining attention in recent years. For example, Fischer's group (Fischer et al. (1999, 2003); Leipner et al. 2000) investigated the behavior of cellulose in a series of MSHs and found that the cellulose dissolved or swollen in MSH, and the crystal forms of cellulose were transformed from cellulose I to cellulose II. Sun et al. (2022) studied the dissolution, regeneration, structure, and morphology of cellulose pretreated with $ZnBr_2{\cdot}RH_2O$ and $FeCl_3{\cdot}RH_2O$, and investigated the influence of dissolution time, temperature, and water content. They found that $ZnBr_2{\cdot}4H_2O$ was a promising and reusable pretreatment solvent for cellulose dissolution. Chen et al. (2020) reported that cellulose could be dissolved fast and efficiently in $ZnCl_2{\cdot}3H_2O$ and $FeCl_3{\cdot}6H_2O$, and proposed the dissolution mechanism of cellulose on the basis of the investigation on the structure of generated cellulose. The dissolution process modified the cellulose structure, leading to the enhancement of cellulose conversion (Lara-Serrano et al. 2020). Various MSHs, especially lithium and zinc-based MSHs, were investigated for cellulose conversion to valuable chemical products. For example, cellulose was efficiently hydrolyzed into glucose and bromo-methylfurfural in acidified LiBr MSH (Yoo et al. 2017b). Levulinic acid (LA) was obtained by converting cellulose in LiCl MSH (Wang et al. 2020). Similarly, cellulose could be converted to glucose (Guan et al. 2021; van den Bergh et al. 2017), isosorbide (Almeida et al. 2010), 1-(furan-2-yl)-2-hydroxyethanone(Yang et al. 2011) and furfural (FF) (Bodachivskyi et al. 2019a, b) in zinc-based MSH.

In MSH, the efficiency of cellulose conversion to glucose is very high, but the yield of further conversion of glucose to 5-hydroxymethylfurfural (HMF) is low, because the efficiency of glucose isomerization is low as the Brønsted acid in MSH is highly strong (Amarasekara and Ebede 2009; Deng et al. 2012; Rodriguez Quiroz et al. 2019b). Additional catalysts (e.g., metals and zeolite) are usually added to MSH to improve the yield of HMF (Wang et al. 2015; Wei and Wu 2017; Yan et al. 2019). In the previous work, the efficiency of cellulose conversion was improved when two kinds of MSH were mixed, illustrating that the mixed MSH was a promising solvent for cellulose dissolution and conversion into invaluable chemicals (Liu et al. 2022). However, the research on cellulose dissolution and conversion into HMF in mixed MSH remains rare, and the understanding on the cooperative catalysis of species in MSH on cellulose conversion is unclear. Therefore, in the present work, the cellulose dissolution and regeneration in a series of MSH were investigated. Basing on the screening of cellulose dissolvability in MSH, cellulose conversion on the mixed MSH ($ZnBr_2{\cdot}3H_2O$–$LiCl{\cdot}3H_2O$) with different $ZnBr_2{\cdot}3H_2O$ concentrations, reaction temperatures, and times was studied. The speciation of $ZnBr_2{\cdot}3H_2O$–$LiCl{\cdot}3H_2O$ was calculated and correlated to HMF yield from fructose conversion. The reaction mechanism for conversion of cellulose into HMF in $ZnBr_2{\cdot}3H_2O$–$LiCl{\cdot}3H_2O$ was also proposed.

Experiment

Materials and reagents

Microcrystalline cellulose (97.0%, particle size 50 μm) was supplied by Yuanye Biotechnology Co., Ltd. Anhydrous inorganic salts lithium chloride (LiCl, 99.0%), zinc bromide($ZnBr_2$, ≥ 98.0%), lithium bromide (LiBr, 99.0%), and methanol(≥ 99.9%) were purchased from Shanghai McLin Biochemical Technology Co., Ltd. Calcium chloride ($CaCl_2$, 99.5%) was obtained from Laiyang Economic Development Zone Chemical Reagent Co., Ltd. Glucose (≥ 99.0%), D-fructose (99.0%), FF (99.0%), LA (99.0%), and HMF (99.0%) were purchased from Aladdin Biochemical Technology Co., Ltd. Methyl isobutyl ketone (MIBK, ≥ 99.0%) was obtained from Tianjin Fucheng Chemical Reagent Co., Ltd.

Cellulose dissolution and regeneration

For pure MSH, the inorganic salt was mixed with deionized water in accordance with the molar ratio of salt/water to obtain MSH. For mixed MSH, it was prepared by mixing two pure MSH with the mass ratio of 1:1. In the experiment, 0.3 g cellulose and 29.7 g MSH were added into a three-necked flask placed in an oil bath equipped with magnetic stirring. The solution was heated at 85 °C for 15 min to dissolve cellulose. After that, cellulose solution was poured into deionized water, and the cellulose was regenerated and diffused in the water. After centrifugal precipitation, the regenerated cellulose was washed with deionized water to remove residual salts, and the sample was centrifuged and freeze-dried before analysis.

Characterization

The X-ray diffraction (XRD) pattern of samples was performed using the D8 ADVANCE from Bruker (Germany) with an operating voltage of 40 kV and a current of 40 mA. The scan range (2θ) was 5°–60° at 2° min^{-1}. The fourier transform infrared (FT-IR) analysis of regenerated cellulose was performed using FT-IR-850 in the range of 500–4000 cm^{-1} at a scan rate of 4 cm^{-1} in the transmission mode. KBr was dried overnight in an oven prior to analysis. ^{13}C NMR spectra were recorded on Bruker Avance III 400 NMR spectrometer.

Cellulose conversion

The conversion of carbohydrates (cellulose, glucose, fructose) in MSH were carried out in a 50 mL Teflon-lined 316 stainless steel autoclave with a mechanical stirrer. Specifically, 0.1 g of microcrystalline cellulose (glucose, fructose) was mixed with 10 g MSH, then 10 mL of MIBK was poured into the autoclave to form biphasic system in order to enhance the production yield. The autoclave was placed and heated in an oil bath with the stirring speed at 500 rpm. Upon completing the reaction, the autoclave was cooled down in a water bath. The reaction solution was centrifuged, the MSH and MIBK phase were separated by using a syringe. The sample from MIBK phase was diluted with methanol and filtered through a nylon organic membrane before analyzing. The MSH phase was washed with deionized water to remove remaining salt, and the cellulose was centrifugated, dried and weighed to calculate the conversion of cellulose. During cellulose conversion, humin, composed of furan rich polymer networks containing different oxygen functional groups, was produced and considered as the byproducts. The presence of humin affects the reusability of MSH, so it has to be removed in the recovery process. For recovery, MSH phase was washed twice with MIBK, and the undesired humins was removed with active carbon. The recovered MSH phase was filtered through a syringe filter to test the recyclability.

Analytical method

Quantitative analysis of liquid samples was conducted using high performance liquid chromatography (HPLC, Shimadzu LC-2030C). The chromatographic equipment was equipped with a UV detector and an analytical column (Welch, Xtimate C18). The elution phase used was methanol–water (*V:V=10:90*) with a flow rate of 0.5 mL·min^{-1}. The column temperature was 30 °C and the maximum absorption wavelength was set at 284 nm. The concentration of the standard sample was measured using HPLC firstly, and then the concentration of product was obtained by using the prepared standard curve of samples. The efficiency of cellulose conversion and the production yields were calculated based on the following equations:

$$Cellulose\ conversion = \frac{m_i^0 - m_i}{m_i^0} \times 100\% \quad (1)$$

$$Yield\ of\ product = \frac{n_j}{n_j^{theroy}} \times 100\% \quad (2)$$

where m_i^0 and m_i are the initial cellulose mass and the mass of remaining cellulose after the reaction; n_j and n_j^{theroy} are the actual moles of product (HMF, FF, LA) in MIBK phase and theory moles of product assuming that cellulose is completely converted.

Results and discussion

Cellulose dissolution and regeneration

The cellulose dissolvability in pure and mixed MSH was investigated. Cellulose was dissolved in $ZnBr_2 \cdot 3H_2O$ and

$LiBr{\cdot}3H_2O$, and swollen in $LiCl{\cdot}3H_2O$ and $CaCl_2{\cdot}3H_2O$. When MSH was mixed, cellulose dissolved in all investigated mixed MSH ($ZnBr_2{\cdot}3H_2O$–$LiCl{\cdot}3H_2O$, $ZnBr_2{\cdot}3H_2O$–$CaCl_2{\cdot}3H_2O$, $LiBr{\cdot}3H_2O$–$LiCl{\cdot}3H_2O$ and $LiBr{\cdot}3H_2O$–$CaCl_2{\cdot}3H_2O$), indicating that mixed MSH was an effective solvent for cellulose dissolution. The dissolution and swelling of cellulose in MSH were summarized in Table 1. Cellulose dissolved in MSH because the hydroxyl group of cellulose interact strongly with the ligand in the cation coordination ring of MSH, causing the hydrogen bonds on cellulose to break (Burchard et al. 1994).

The XRD patterns and FT-IR spectra of raw and regenerated celluloses from MSH were analyzed to elucidate the structural change and the interaction of cellulose and MSH. In Fig. 1A, raw cellulose showed distinct characteristic peaks at 14.7°, 16.4°, 22.3°, and 34.5° (curve *a*), which represent the structural characteristic peaks of cellulose I (Hao et al. 2015; Huang et al. 2020; Sun et al. 2016). Regenerated cellulose treated with $ZnBr_2{\cdot}3H_2O$ (curve *d*) exhibited three peaks at 12.3°, 20.2°, and 22.3°, which were the characteristic peaks of cellulose II, demonstrating that structure of cellulose was changed during regeneration process (Liu et al. 2015). The XRD patterns of celluloses regenerated from $LiCl{\cdot}3H_2O$ (curve *b*) and $CaCl_2{\cdot}3H_2O$ (curve *c*) showed characteristic peaks of both cellulose I and II, indicating that partial dissolution occurred when cellulose was swollen in MSH (Nam et al. 2016). The XRD pattern of celluloses regenerated from $LiBr{\cdot}3H_2O$ (curve *e*) showed an amorphous structure, demonstrating that the structure of cellulose was destroyed and could not be reformed during regeneration process. The XRD patterns of the regenerated cellulose from mixed MSH displayed cellulose II at 12.3°, 20.2°, and 22.3° in Fig. 1B. The results showed that the structure of cellulose was destroyed in mixed MSH and different hydrogen bonds were formed during regeneration (Wohlert et al. 2022).

Table 1 MSH for dissolution and swelling of cellulose

	Pure MSH	Mixed MSH
Dissolution	$LiBr{\cdot}3H_2O$	$LiBr{\cdot}3H_2O$–$LiCl{\cdot}3H_2O$, $LiBr{\cdot}3H_2O$–$CaCl_2{\cdot}3H_2O$
	$ZnBr_2{\cdot}3H_2O$	$ZnBr_2{\cdot}3H_2O$–$LiCl{\cdot}3H_2O$, $ZnBr_2{\cdot}3H_2O$–$CaCl_2{\cdot}3H_2O$
Swelling	$LiCl{\cdot}3H_2O$	
	$CaCl_2{\cdot}3H_2O$	

The FT-IR profiles of the raw and regenerated celluloses were investigated. The peak at 3700–3000 cm^{-1} was assigned to the vibration of the O–H stretching vibration of cellulose. The peak at 1639 cm^{-1} was attributed to the vibration of molecular water. The peaks at 1430 and 1112 cm^{-1} represent the H-C-H bending vibration and the C–OH backbone vibration in cellulose, respectively. As shown in Fig. 1C, the peaks at 1430 and 1112 cm^{-1} disappeared for cellulose regenerated with $ZnBr_2{\cdot}3H_2O$ and $LiBr{\cdot}3H_2O$ (curves *d* and *e*), indicating that the cellulose structure was changed during the dissolution process and the cellulose type I structure was altered. In contrast, for cellulose regenerated with $CaCl_2{\cdot}3H_2O$ (curve *c*), the peak only at 1112 cm^{-1} disappeared, indicating that partial dissolution of cellulose occurred. The peaks at 2900 and 897 cm^{-1} were attributed to -CH_2-alkyl stretching vibration and *β*-glucosidic linkages between the sugar units, respectively, and no significant differences were found, suggesting that no further degradation of cellulose occurs in MSH. As shown in Fig. 1D, the vibration peaks of all regenerated celluloses disappeared at 1430 and 1112 cm^{-1}, indicating that the cellulose type I structure was disrupted. The peak of C–O–C pyranose ring skeletal vibrations at 1053 cm^{-1} was weak in the regenerated celluloses from $LiBr{\cdot}3H_2O$–$CaCl_2{\cdot}3H_2O$ (curve *h*) and $LiBr{\cdot}3H_2O$–$LiCl{\cdot}3H_2O$ (curve *i*). This phenomenon suggested that the structure of cellulose changed during the dissolution and regeneration process.

When MSH was mixed, the interactions among inorganic salt, water, and cellulose were complex, and the dissolution properties of cellulose were changed. It was not destructive to the cellulose crystal form as the regenerated cellulose exhibited the structure of cellulose II. However, the bonds of the regenerated cellulose changed especially the H–C–H and C–OH bonds, remarkably.

Cellulose conversion

Cellulose conversion could be used to prepare glucose, HMF, FF, LA, and other high value-added chemicals (Silva Lacerda et al. 2015; Fidio et al.

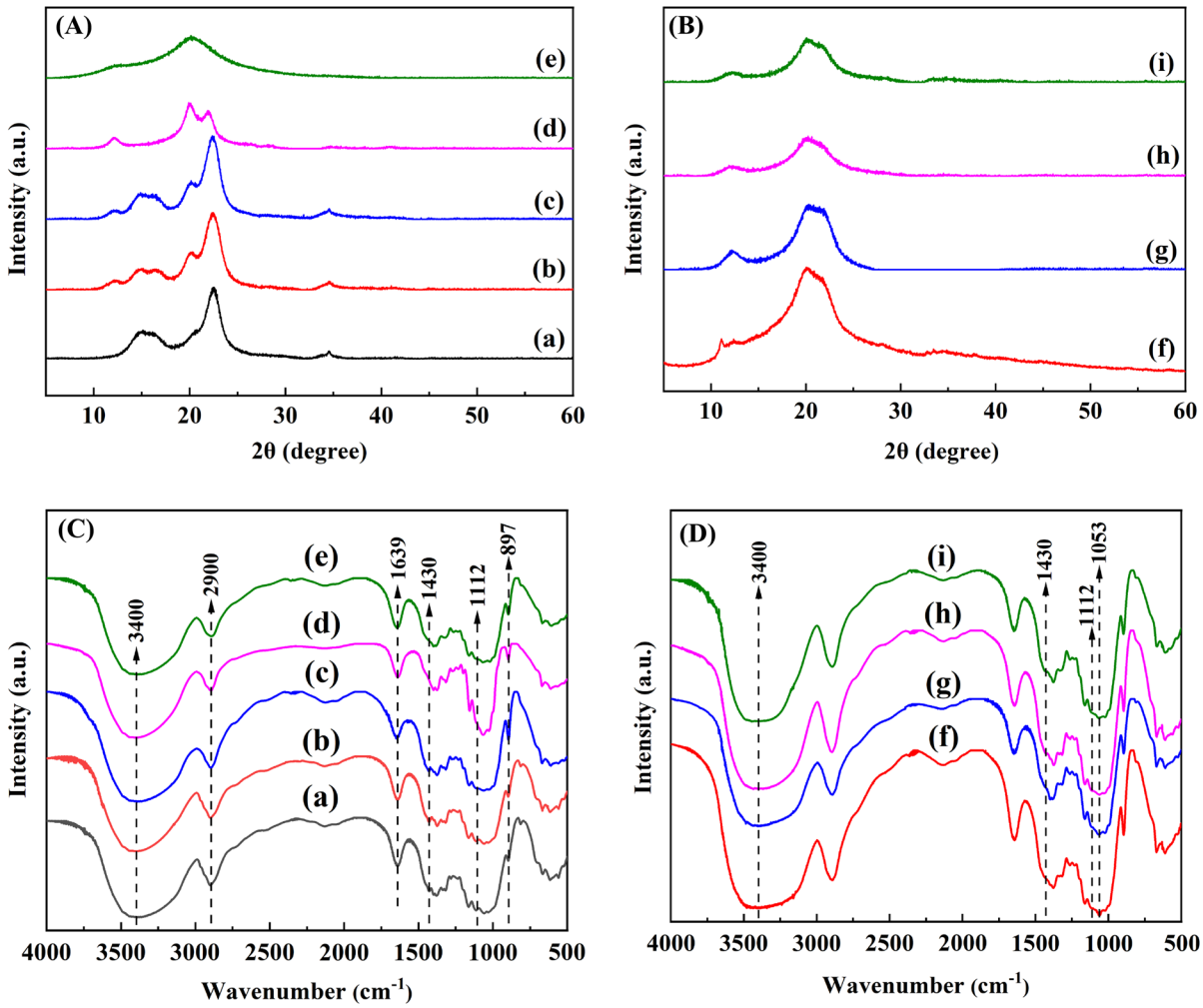

Fig. 1 (**A**) and (**B**) XRD patterns; (**C**) and (**D**) FTIR spectra. Curves: (**a**) raw cellulose; cellulose regenerated from (**b**) $LiCl{\cdot}3H_2O$; (**c**) $CaCl_2{\cdot}3H_2O$; (**d**) $ZnBr_2{\cdot}3H_2O$; (**e**) $LiBr{\cdot}3H_2O$; (**f**) $ZnBr_2{\cdot}3H_2O$–$CaCl_2{\cdot}3H_2O$; (**g**) $ZnBr_2{\cdot}3H_2O$–$LiCl{\cdot}3H_2O$; (**h**) $LiBr{\cdot}3H_2O$–$CaCl_2{\cdot}3H_2O$; (**i**) $LiBr{\cdot}3H_2O$–$LiCl{\cdot}3H_2O$

2020). It was reported that carbohydrates can be converted into valuable chemicals in zinc-based MSH (Guan et al. 2021; Deng et al. 2015), LiBr MSH (Yoo et al. 2017b), LiCl MSH (Wang et al. 2020) and $CaCl_2$ MSH (Lin et al. 2021). However, it was found that the efficiency of cellulose conversion into HMF was low in single MSH. Therefore, mixed MSHs were prepared by mixing two kinds of single-MSH with a mass ratio of 1:1 and screened for conversion of cellulose in this work. The efficiencies of cellulose conversion were investigated in $ZnBr_2{\cdot}3H_2O$–$CaCl_2{\cdot}3H_2O$, $ZnBr_2{\cdot}3H_2O$–$LiCl{\cdot}3H_2O$, $ZnBr_2{\cdot}3H_2O$–$LiBr{\cdot}3H_2O$, $LiBr{\cdot}3H_2O$–$CaCl_2{\cdot}3H_2O$ and $LiBr{\cdot}3H_2O$–$LiCl{\cdot}3H_2O$. The results showed that cellulose was almost completely converted, and the yields of products, including HMF, FF, and LA were high in $ZnBr_2{\cdot}3H_2O$–$LiCl{\cdot}3H_2O$ and $ZnBr_2{\cdot}3H_2O$–$LiBr{\cdot}3H_2O$ (Fig. S1). The HMF yield was relatively high in $ZnBr_2{\cdot}3H_2O$–$LiCl{\cdot}3H_2O$, and conducive to the formation of FF in $ZnBr_2{\cdot}3H_2O$–$LiBr{\cdot}3H_2O$.

Based on the investigation on cellulose dissolution and conversion in mixed MSH, $ZnBr_2{\cdot}3H_2O$–$LiCl{\cdot}3H_2O$ was found to be a good dissolving agent and effective catalyst for cellulose conversion. The $ZnBr_2{\cdot}3H_2O$ concentration, reaction temperature, and time were optimized to obtain

high HMF yield. Figure 2A showed the influence of $ZnBr_2{\cdot}3H_2O$ concentration on product yield at 180 °C and 60 min. The yields of HMF in pure $LiCl{\cdot}3H_2O$ and pure $ZnBr_2{\cdot}3H_2O$ were low, which were only 8.3% and 1.86%, respectively. Studies showed that $ZnBr_2{\cdot}3H_2O$ could dissolve cellulose and efficiently convert cellulose into glucose (Sadula et al. 2021). However, the yield of products, such as HMF, was low due to the inefficiency of glucose isomerization. When $ZnBr_2{\cdot}3H_2O$ and $LiCl{\cdot}3H_2O$ were mixed, the yield of HMF increased significantly, reaching the maximum at 60 wt.% $ZnBr_2{\cdot}3H_2O$, because the concentration of Lewis acids in the system increased, and the isomerization efficiency was enhanced, which was proven by the increase in FF and LA yields (Liu et al. 2022; Yoo et al. 2017a). The maximum yield of products, including HMF, LA, and FF, reached 75% in $ZnBr_2{\cdot}3H_2O$–$LiCl{\cdot}3H_2O$ when the mass fraction of $ZnBr_2{\cdot}3H_2O$ was 60 wt.%. As the $ZnBr_2{\cdot}3H_2O$ concentration continued to increase (60 wt.%–100 wt.%), excessive byproducts, such as humins, were generated in the system, leading to decreased HMF yield (Tyagi et al. 2019), which could be clearly identified by the color of production's photograph (Fig. S2). In $ZnBr_2{\cdot}3H_2O$–$LiCl{\cdot}3H_2O$ system, the metal-contained species acted as the Lewis acids and the hydrolyzed hydrogen ion acted as the Brønsted acid. The conversion of cellulose to HMF required the cooperative catalysis of Lewis and Brønsted acids (Hafizi et al. 2022). The HMF yield increased when $ZnBr_2{\cdot}3H_2O$ was mixed with $LiCl{\cdot}3H_2O$ in a certain proportion as sufficient Lewis and Brønsted acid catalytic active centers were provided.

Figure 2B showed the effect of reaction temperature on cellulose conversion into HMF in $ZnBr_2{\cdot}3H_2O$–$LiCl{\cdot}3H_2O$. The yield of HMF in the

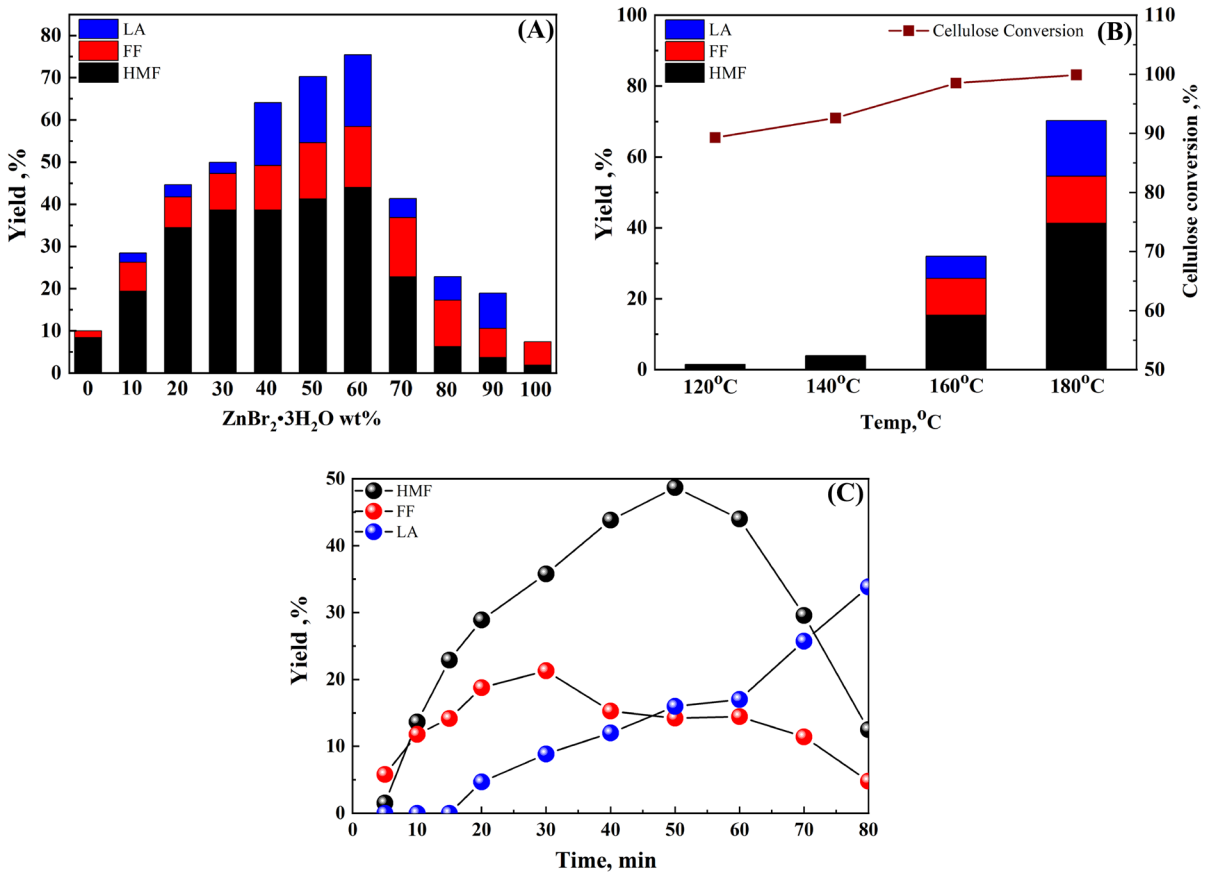

Fig. 2 Cellulose conversion in $ZnBr_2{\cdot}3H_2O$–$LiCl{\cdot}3H_2O$: (**A**) effect of $ZnBr_2{\cdot}3H_2O$ concentration at 180 °C for 60 min; (**B**) effect of temperature in 60 wt.% $ZnBr_2{\cdot}3H_2O$ for 60 min; (**C**) effect of reaction time in 60 wt.% $ZnBr_2{\cdot}3H_2O$ at 180 °C

system was quite low at 120 °C and 140 °C, which has been demonstrated in the literatures that cellulose was converted to glucose at these temperatures (Lara-Serrano et al. 2020; Yu et al. 2018). The cellulose conversion and production yield increased gradually with increasing temperature, and the highest value was reached at 180 °C.

The influence of reaction time on cellulose conversion was shown in Fig. 2C. At the initial 50 min, the HMF and LA yields increased progressively. With prolonged reaction time, the HMF yield decreased, whereas the LA yield increased. The reason was that cellulose was dissolved in mixed MSH at the beginning of the reaction. This phenomenon accelerated the conversion of cellulose into HMF, which was unstable and tended to continue to be rehydrated to LA as time went on. At 80 min, LA became the main product, and the yield reached 33.8%. The trend of FF yield was similar to that of HMF, that was, increased first and then decreased with time.

Glucose and fructose conversion

The conversion of cellulose into HMF and FF includes cellulose dissolution and hydrolysis, glucose isomerization, and fructose conversion. Cellulose could be dissolved quickly and hydrolyzed efficiently to glucose in $ZnBr_2{\cdot}3H_2O$–$LiCl{\cdot}3H_2O$. Subsequently, the conversion of glucose and fructose played an important role in the yield and selectivity of the product (Qi et al. 2019). The isomerization of glucose to fructose was investigated and the result was shown in Fig S3. Both the glucose conversion and fructose yield were high in $ZnBr_2{\cdot}3H_2O$–$LiCl{\cdot}3H_2O$, which was consistent with the trend of product yield from cellulose conversion and proved that glucose isomerization was the control step of cellulose conversion. In view of this, the ^{13}C-NMR spectra of chemicals obtained from the conversion of glucose and fructose in $ZnBr_2{\cdot}3D_2O$–$LiCl{\cdot}3D_2O$ were collected to gain insights into the pathways of glucose isomerization. As shown in Fig. 3, curves *a* and *b* were the ^{13}C NMR spectra of glucose and fructose, and curves *c* and *d* were the ^{13}C NMR spectra of glucose and fructose in $ZnBr_2{\cdot}3D_2O$–$LiCl{\cdot}3D_2O$. The presence of fructose was corroborated by the appearance of resonance at $\delta = 98$, 69.1, and 64.1 ppm in the ^{13}C NMR spectrum when glucose was isomerized in $ZnBr_2{\cdot}3D_2O$–$LiCl{\cdot}3D_2O$ in curve *c* (Yoo et al. 2017a). The low strength of resonance could be attributed to the low proportion of fructose in the reaction of glucose isomerization. The peaks at 64.5 and 70.4 ppm were observed in curve *d*, illustrating that arabinose was formed during the conversion of fructose. Thus, fructose and arabinose were produced in the process of glucose conversion.

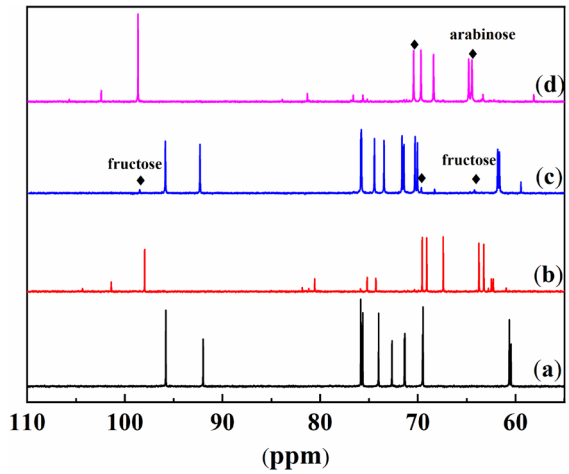

Fig. 3 ^{13}C NMR spectra of (**a**) glucose, (**b**) fructose, (**c**) glucose in $ZnBr_2{\cdot}3D_2O$–$LiCl{\cdot}3D_2O$, (**d**) fructose in $ZnBr_2{\cdot}3D_2O$–$LiCl{\cdot}3D_2O$

For further research, the conversions of glucose and fructose were investigated at different $ZnBr_2{\cdot}3H_2O$ concentrations, reaction temperatures, and times. As shown in Fig. 4A, the yield of HMF from glucose conversion in $LiCl{\cdot}3H_2O$ was only 13.4%. When the concentration of $ZnBr_2{\cdot}3H_2O$ was 40 wt.%, the yield of HMF reached a maximum of 43.9%. From 0 to 40 wt.% $ZnBr_2{\cdot}3H_2O$ concentration, the yield of HMF increased with increasing $ZnBr_2{\cdot}3H_2O$ concentration, whereas the yield of FF slightly changed. Afterwards, the HMF yield decreased, and the FF yield increased with increasing $ZnBr_2{\cdot}3H_2O$ concentration, showing that a competitive reaction existed in the generation of HMF and FF. For fructose conversion, the HMF and FF yields increased and then decreased with increasing $ZnBr_2{\cdot}3H_2O$ concentration (Fig. 4B).

Based on the above analysis, the conversion of glucose to HMF and FF in $ZnBr_2{\cdot}3H_2O$–$LiCl{\cdot}3H_2O$ involves two paths: (1) glucose isomerization into fructose and fructose dehydration into HMF; (2) glucose isomerization into fructose, fructose conversion

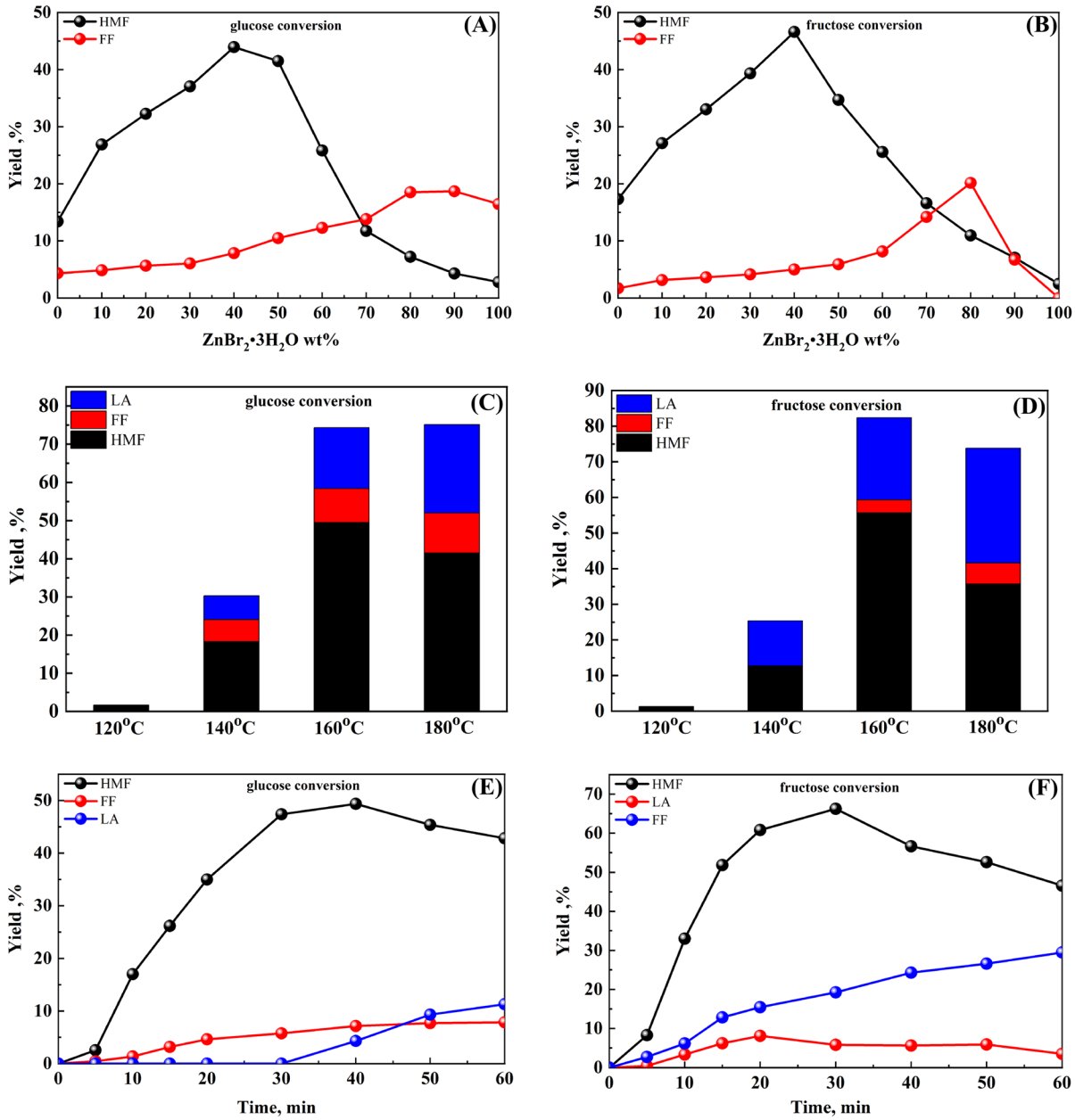

Fig. 4 Production yield in $ZnBr_2{\cdot}3H_2O$–$LiCl{\cdot}3H_2O$ from glucose and fructose conversion: (**A**), (**B**) effect of $ZnBr_2{\cdot}3H_2O$ concentration at 180 °C for 60 min; (**C**), (**D**) effect of temperature in 50 wt.% $ZnBr_2{\cdot}3H_2O$ for 60 min; (**E**), (**F**) effect of reaction time in 60 wt.% $ZnBr_2{\cdot}3H_2O$ at 180 °C

into arabinose, and arabinose dehydration into FF. Fructose conversion into HMF and FF was catalyzed by different species in $ZnBr_2{\cdot}3H_2O$–$LiCl{\cdot}3H_2O$. When the concentration of $ZnBr_2{\cdot}3H_2O$ was lower than 80 wt.%, the trend of production yield of HMF and FF from glucose conversion was similar to that from fructose conversion, indicating that the species that catalyzed the two paths were sufficient. When the concentration of $ZnBr_2{\cdot}3H_2O$ was high (> 80 wt.%), the conversion of fructose was inefficient, resulting in decreased FF yield.

The effects of temperature in the conversion of glucose and fructose to HMF were shown in Fig. 4C and D. The HMF yield increased when the temperature was increased from 120 °C to 160 °C. As the temperature was increased to 180 °C, the HMF yield decreased due to the enhancement of LA, demonstrating that high temperature facilitated the production of LA. Figures 4E and F showed the effects of reaction time on glucose and fructose conversion into HMF in 60 wt.% $ZnBr_2{\cdot}3H_2O$–$LiCl{\cdot}3H_2O$. The yield of HMF converted from glucose increased progressively at the initial 40 min and then decreased with prolonged reaction time from 40 to 60 min. The decrease was caused by the generation of byproducts, such as LA, FF, and humins. The yield of HMF for fructose conversion reached the maximum (66.2%) at 30 min. As the reaction continued, the yield of HMF gradually decreased.

Cooperative catalysis of species in MSH

Given the complexity of species and the difficulty in determining the concentration of species, the Lewis and Brønsted acids required for catalytic reaction could not be accurately regulated, resulting in low catalytic efficiency. Therefore, in this work, the concentrations of species in $ZnBr_2{\cdot}3H_2O$–$LiCl{\cdot}3H_2O$ were calculated using the OLI software on the basis of the aqueous thermodynamic framework to explain the effect of species on the reaction, and the complex aqua-species coordinate was represented as $Zn(OH)_x^{2-x}$ for simplicity. As shown in Fig. 5A, the Li^+ and Cl^- concentrations decreased with increasing $ZnBr_2{\cdot}3H_2O$ concentration. The Br^- concentration changed in a wavy manner. The concentrations of Zn^{2+}, $ZnCl^+$, and $ZnBr^+$ increased sharply when the concentration of $ZnBr_2{\cdot}3H_2O$ was larger than 70 wt.%, whereas these concentrations were quite low at low $ZnBr_2{\cdot}3H_2O$ concentration. The concentration of $ZnCl_3^-$ increased and then decreased with maximum peaks at 70 wt.% $ZnBr_2{\cdot}3H_2O$. Combined with the conversion experiment of glucose and fructose, the yield of FF was gradually higher than that of HMF when $ZnBr_2{\cdot}3H_2O$ was larger than 70 wt.%, further indicating that the formation of FF and HMF was closely related to the concentration of species in the system.

The relationship between the ion concentration in $ZnBr_2{\cdot}3H_2O$–$LiCl{\cdot}3H_2O$ and the production yield obtained from the conversion of fructose was studied to elucidate the mechanism for cellulose conversion. As shown in Fig. 5B, the HMF yield obtained from fructose was linearly correlated with the functions of H^+ and Br^- concentrations ($c_{Br^-}+10^4 c_{H^+}$), and the FF yield from fructose conversion was linearly related with the concentration of H^+ and $ZnBr_3^-$ in $ZnBr_2{\cdot}3H_2O$–$LiCl{\cdot}3H_2O$ ($c_{ZnBr_3^-}+2*10^4 c_{H^+}$).

Based on the experiments on cellulose/glucose/fructose conversion, NMR characterization and thermodynamic calculation, the

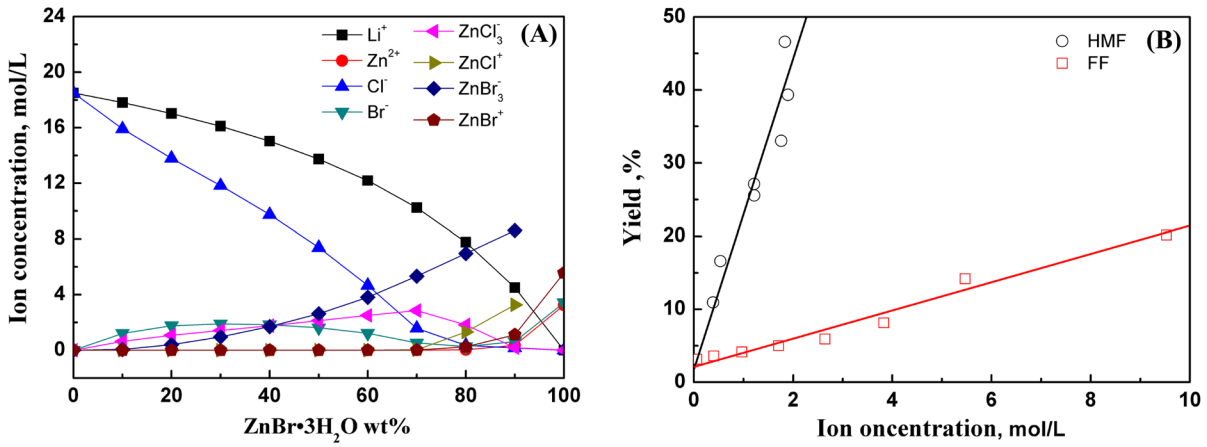

Fig. 5 (**A**) The species concentrations in $ZnBr_2{\cdot}3H_2O$–$LiCl{\cdot}3H_2O$; (**B**) fructose conversion to HMF and FF versus the function of species concentrations

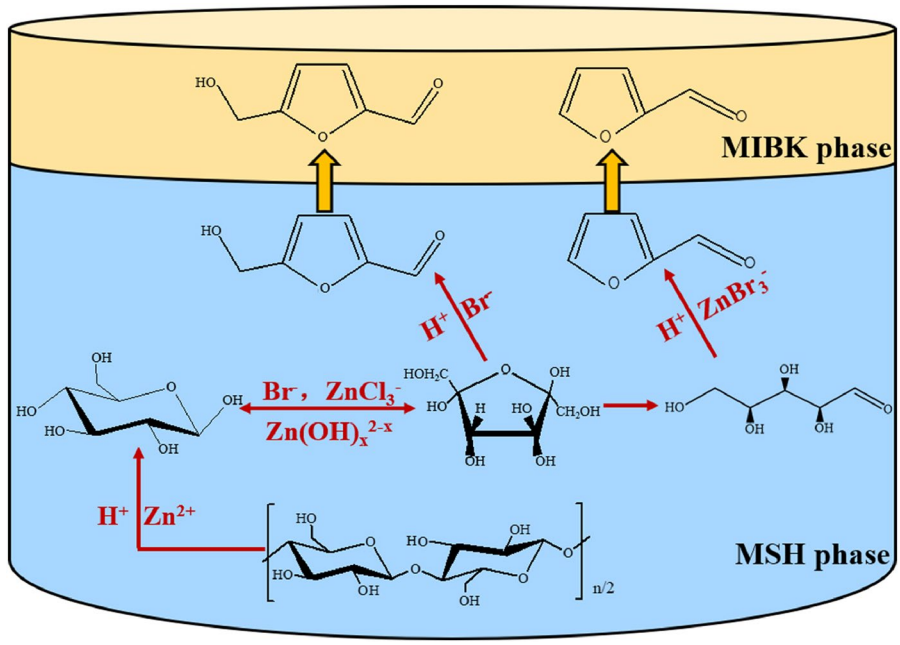

Fig. 6 Proposed mechanism for cellulose conversion in $ZnBr_2{\cdot}3H_2O$–$LiCl{\cdot}3H_2O$

mechanism for converting cellulose into HMF in $ZnBr_2{\cdot}3H_2O$–$LiCl{\cdot}3H_2O$ was proposed, as shown in Fig. 6. A biphasic system MIBK/MSH was used to extract the product from the cellulose conversion to minimize the generation of side reactions and increase the product yield. In the process of cellulose conversion, cellulose was first dissolved and hydrolyzed to glucose under the interaction of H^+ and Zn^{2+}. Then, glucose was isomerized into fructose by the catalysis of Br^-, $ZnCl_3^-$, and $Zn(OH)_x^{2-x}$. These species acted as Lewis acid and interacted with the oxygen atoms in glucose. The efficiency of glucose isomerization was improved by increasing the concentration of active species when $LiCl{\cdot}3H_2O$ was mixed with $ZnBr_2{\cdot}3H_2O$. Finally, fructose was dehydrated to HMF catalyzed by H^+ and Br^- and converted FF catalyzed by H^+ and $ZnBr_3^-$. The type and concentration of species have an important effect on the yield and selectivity of products. The high-efficiency conversion of cellulose to valuable chemicals could be realized by adjusting the species in the MSH.

Recycling of MSH

The recycling test for cellulose conversion into HMF in $ZnBr_2{\cdot}3H_2O$–$LiCl{\cdot}3H_2O$ was carried out to examine the reusability of MSH, as shown in Fig. 7.

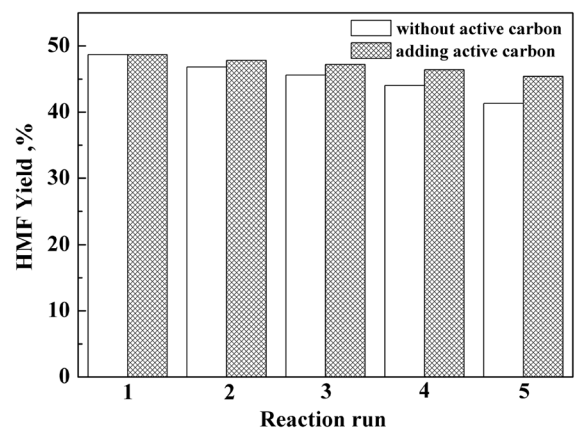

Fig. 7 Recycling performance for cellulose conversion in $ZnBr_2{\cdot}3H_2O$–$LiCl{\cdot}3H_2O$. Conditions: 0.1 g cellulose, 10 g MSH, 5 g active carbon, 10 mL MIBK, 60 wt.% $ZnBr_2{\cdot}3H_2O$, 180 °C, 50 min

After each cycle, MSH was recovered by separating MSH from the organic phase, washed with MIBK, and used directly for next run. The results showed that HMF yield dropped from 48.7 to 41.3% after five cycles. The reason was that humins were produced in the reaction after each run and MSH phase became darker and darker. Considering this, activated carbon was added to the MSH recovery process to adsorb produced humins after each run, and the yield of HMF decreased slightly from 48.7 to

45.4%. The decline was unnoticeable, suggesting that $ZnBr_2{\cdot}3H_2O$–$LiCl{\cdot}3H_2O$ is reusable for cellulose conversion into HMF.

Conclusions

In this work, cellulose dissolution and conversion into HMF in different MSHs were systematically investigated. $ZnBr_2{\cdot}3H_2O$–$LiCl{\cdot}3H_2O$ was found to be an efficient solvent and catalyst for cellulose conversion. Mixed MSH significantly improved the efficiency of cellulose conversion into HMF. The species in the system cooperated to catalyze the efficient conversion of cellulose, and the yield of HMF was reached 48.7% at 60 wt.% $ZnBr_2{\cdot}3H_2O$ under optimal conditions. Experimental results and species calculations demonstrated that Br^- and H^+ catalyzed the conversion of fructose to HMF, while $ZnBr_3^-$ and H^+ promoted the conversion of fructose into arabinose, which promoted the formation of FF, competing with the production of HMF. This work gave insight into the cooperative catalysis of species in mixed MSH and laid the foundation for the efficient conversion of cellulose and related biomass to valuable chemicals in MSH.

Acknowledgments The authors are thankful for financial supports from National Natural Science Foundation of China (No. 21978158, 22078180 and 21878143), the National Key Research and Development Program of China (No. 2019YFD1100602), and SDUT & Zhangdian Integration Development Project (No. 2021JSCG0010).

Author contributions CW: Investigation, Writing–original draft; GL: Investigation, Data curation; YX: Supervision, Methodology, Writing–review & editing; ZS: Investigation, Data curation; CL: Software; FS: Funding acquisition; HC: Methodology, Funding acquisition, Writing – review & editing.

Funding This work was supported by National Natural Science Foundation of China (No. 21978158, 22078180 and 21878143), the National Key Research and Development Program of China (No. 2019YFD1100602), and SDUT & Zhangdian Integration Development Project (No. 2021JSCG0010).

Data availability The data supporting this study are available when reasonably requested from the corresponding author.

Declarations

Conflict of interests The authors have no relevant financial or non-financial interests to disclose.

Consent to participate Informed consent was obtained from all participants included in the study.

Consent for publication Informed consent was obtained from all participants for publication.

References

Ab Rasid NS, Shamjuddin A, Abdul Rahman AZ, Amin NAS (2021) Recent advances in green pre-treatment methods of lignocellulosic biomass for enhanced biofuel production. J Clean Prod 321:129038. https://doi.org/10.1016/j.jclepro.2021.129038

Almeida RM, Li J, Nederlof C, O'Connor P, Makkee M, Moulijn JA (2010) Cellulose conversion to isosorbide in molten salt hydrate media. Chemsuschem 3:325–328. https://doi.org/10.1002/cssc.200900260

Amarasekara AS, Ebede CC (2009) Zinc chloride mediated degradation of cellulose at 200°C and identification of the products. Bioresour Technol 100:5301–5304. https://doi.org/10.1016/j.biortech.2008.12.066

Ashokkumar V, Venkatkarthick R, Jayashree S, Chuetor S, Dharmaraj S, Kumar G, Chen WH, Ngamcharussrivichai C (2021) Recent advances in lignocellulosic biomass for biofuels and value-added bioproducts - A critical review. Bioresour Technol. https://doi.org/10.1016/j.biortech.2021.126195

Bodachivskyi I, Kuzhiumparambil U, Williams DBG (2019a) Acid-catalysed conversion of carbohydrates into furan-type molecules in zinc chloride hydrate. ChemPlusChem 84:352–357. https://doi.org/10.1002/cplu.201800650

Bodachivskyi I, Kuzhiumparambil U, Williams DBG (2019b) The role of the molecular formula of $ZnCl_2{\cdot}nH_2O$ on its catalyst activity: a systematic study of zinc chloride hydrates in the catalytic valorisation of cellulosic biomass. Catal Sci Technol 9:4693–4701. https://doi.org/10.1039/C9CY00846B

Burchard W, Habermann N, Klüfers P, Seger B, Wilhelm U (1994) Cellulose in Schweizer's reagent: A stable, polymeric metal complex with high chain stiffness. Angew Chem Int Edit 33:884–887. https://doi.org/10.1002/anie.199408841

Chen Y, Yu H-Y, Li Y (2020) Highly efficient and superfast cellulose dissolution by green chloride salts and its dissolution mechanism. ACS Sustain Chem Eng 8:18446–18454. https://doi.org/10.1021/acssuschemeng.0c05788

Cho EJ, Trinh LTP, Song Y, Lee YG, Bae HJ (2020) Bioconversion of biomass waste into high value chemicals. Bioresour Technol 298:122386. https://doi.org/10.1016/j.biortech.2019.122386

Deng T, Cui X, Qi Y, Wang Y, Hou X, Zhu Y (2012) Conversion of carbohydrates into 5-hydroxymethylfurfural catalyzed by $ZnCl_2$ in water. Chem Commun 48:5494–5496. https://doi.org/10.1039/C2CC00122E

Deng W, Kennedy JR, Tsilomelekis G, Zheng W, Nikolakis V (2015) Cellulose hydrolysis in acidified LiBr molten salt hydrate media. Ind Eng Chem Res 54:5226–5236. https://doi.org/10.1039/C2CC00122E

Emons H (1988) Structure and properties of molten salt hydrates. Electrochim Acta 33:1243–1250. https://doi.org/10.1016/0013-4686(88)80155-5

Feng L, Chen ZL (2008) Research progress on dissolution and functional modification of cellulose in ionic liquids. J Mol Liq 142:1–5. https://doi.org/10.1016/j.molliq.2008.06.007

Fidio N, Fulignati S, De Bari I, Antonetti C, Raspolli Galletti AM (2020) Optimization of glucose and levulinic acid production from the cellulose fraction of giant reed (Arundo donax L) performed in the presence of ferric chloride under microwave heating. Bioresour Technol 313:123650. https://doi.org/10.1016/j.biortech.2020.123650

Fischer S, Voigt W, Fischer K (1999) The behaviour of cellulose in hydrated melts of the composition $LiX{\cdot}nH_2O$ ($X=I^-$, NO_3^-, CH_3COO^-, ClO_4^-). Cellulose 6:213–219. https://doi.org/10.1023/A:1009269614096

Fischer S, Leipner H, Thümmler K, Brendler E, Peters J (2003) Inorganic molten salts as solvents for cellulose. Cellulose 10:227–236. https://doi.org/10.1023/A:1025128028462

Guan M, Liu Q, Xin H, Jiang E, Ma Q (2021) Enhanced glucose production from cellulose and corn stover hydrolysis by molten salt hydrates pretreatment. Fuel Process Technol 215:106739. https://doi.org/10.1016/j.fuproc.2021.106739

Hafizi H, Walker G, Collins MN (2022) Efficient production of 5-ethoxymethylfurfural from 5-hydroxymethylfurfural and carbohydrates over lewis/brønsted hybrid magnetic dendritic fibrous silica core-shell catalyst. Renew Energ 183:459–471. https://doi.org/10.1016/j.renene.2021.11.036

Hao X, Shen W, Chen Z, Zhu J, Feng L, Wu Z, Wang P, Zeng X, Wu T (2015) Self-assembled nanostructured cellulose prepared by a dissolution and regeneration process using phosphoric acid as a solvent. Carbohyd Polym 123:297–304. https://doi.org/10.1016/j.carbpol.2015.01.055

Huang Z, Liu C, Feng X, Wu M, Tang Y, Li B (2020) Effect of regeneration solvent on the characteristics of regenerated cellulose from lithium bromide trihydrate molten salt. Cellulose 27:9243–9256. https://doi.org/10.1007/s10570-020-03440-y

Lara-Serrano M, Morales-delaRosa S, Campos-Martín JM, Fierro JLG (2020) High enhancement of the hydrolysis rate of cellulose after pretreatment with inorganic salt hydrates. Green Chem 22:3860–3866. https://doi.org/10.1039/D0GC01066A

Leipner H, Fischer S, Brendler E, Voigt W (2000) Structural changes of cellulose dissolved in molten salt hydrates. Macromol Chem Phys 201:2041–2049. https://doi.org/10.1002/1521-3935(20001001)201:15%3c2041::AID-MAPCP2041%3e3.0

Lin C, Chai C, Li Y, Chen J, Lu Y, Wu H, Zhao L, Cao F, Chen K, Wei P, Ouyang P (2021) $CaCl_2$ molten salt hydrate-promoted conversion of carbohydrates to 5-hydroxymethylfurfural: an experimental and theoretical study. Green Chem 23(5):2058–2068. https://doi.org/10.1039/D0GC04356G

Liu Z, Sun X, Hao M, Huang C, Xue Z, Mu T (2015) Preparation and characterization of regenerated cellulose from ionic liquid using different methods. Carbohyd Polym 117:99–105. https://doi.org/10.1016/j.carbpol.2014.09.053

Liu G, Xie Y, Wei C, Liu C, Song F, Sun X, Zhang Y, Cui H (2022) Synergistic catalysis of species in molten salt hydrate for conversion of cellulose to 5-hydroxymethylfurfural. Biomass Bioenerg 158:106363. https://doi.org/10.1016/j.biombioe.2022.106363

Nam S, French AD, Condon BD, Concha M (2016) Segal crystallinity index revisited by the simulation of X-ray diffraction patterns of cotton cellulose Iβ and cellulose II. Carbohyd Polym 135:1–9. https://doi.org/10.1016/j.carbpol.2015.08.035

Qi T, He M, Zhu L, Lyu YJ, Hu CW (2019) Cooperative catalytic performance of lewis and bronsted acids from $AlCl_3$ salt in aqueous solution toward glucose-to-fructose isomerization. J Phys Chem C 123:4879–4891. https://doi.org/10.1021/acs.jpcc.8b11773

Rodriguez Quiroz N, Norton AM, Nguyen H, Vasileiadou E, Vlachos DG (2019a) Homogeneous metal salt solutions for biomass upgrading and other select organic reactions. ACS Catal 9:9923–9952. https://doi.org/10.1021/acscatal.9b01853

Rodriguez Quiroz N, Padmanathan AMD, Mushrif SH, Vlachos DG (2019b) Understanding acidity of molten salt hydrate media for cellulose hydrolysis by combining kinetic studies, electrolyte solution modeling, molecular dynamics simulations, and ^{13}C NMR experiments. ACS Catal 9:10551–10561. https://doi.org/10.1021/acscatal.9b03301

Sadula S, Rodriguez Quiroz N, Athaley A, Ebikade EO, Ierapetritou M, Vlachos DG, Saha B (2021) One-step lignocellulose depolymerization and saccharification to high sugar yield and less condensed isolated lignin. Green Chem 23:1200–1211. https://doi.org/10.1039/D0GC04119J

Silva Lacerda V, López-Sotelo JB, Correa-Guimarães A, Hernández-Navarro S, Sánchez-Bascones M, Navas-Gracia LM, Martín-Ramos P, Pérez-Lebeña E, Martín-Gil J (2015) A kinetic study on microwave-assisted conversion of cellulose and lignocellulosic waste into hydroxymethylfurfural/furfural. Bioresour Technol 180:88–96. https://doi.org/10.1016/j.biortech.2014.12.089

Sun B, Zhang M, Hou Q, Liu R, Wu T, Si C (2016) Further characterization of cellulose nanocrystal (CNC) preparation from sulfuric acid hydrolysis of cotton fibers. Cellulose 23:439–450. https://doi.org/10.1007/s10570-015-0803-z

Sun L, Han J, Wu J, Huang W, Li Y, Mao Y, Wang L, Wang Y (2022) Cellulose pretreatment with inorganic salt hydrate: dissolution, regeneration, structure and morphology. Ind Crop Prod 180:114722. https://doi.org/10.1016/j.indcrop.2022.114722

Tyagi U, Anand N, Kumar D (2019) Simultaneous pretreatment and hydrolysis of hardwood biomass species catalyzed by combination of modified activated carbon and ionic liquid in biphasic system. Bioresour Technol 289:121675. https://doi.org/10.1016/j.biortech.2019.121675

Van den Bergh J, Babich IV, O'Connor P, Moulijn JA (2017) Production of monosugars from lignocellulosic biomass in molten salt hydrates: Process design and techno-economic

analysis. Ind Eng Chem Res 56:13423–13433. https://doi.org/10.1021/acs.iecr.7b01018

Wang Y, Pedersen CM, Qiao Y, Deng T, Shi J, Hou X (2015) In situ NMR spectroscopy: inulin biomass conversion in $ZnCl_2$ molten salt hydrate medium—$SnCl_4$ addition controls product distribution. Carbohyd Polym 115:439–443. https://doi.org/10.1016/j.carbpol.2014.09.011

Wang J, Cui H, Wang Y, Zhao R, Xie Y, Wang M, Yi W (2020) Efficient catalytic conversion of cellulose to levulinic acid in the biphasic system of molten salt hydrate and methyl isobutyl ketone. Green Chem 22:4240–4251. https://doi.org/10.1039/D0GC00897D

Wei W, Wu S (2017) Depolymerization of cellulose into high-value chemicals by using synergy of zinc chloride hydrate and sulfate ion promoted titania catalyst. Bioresour Technol 241:760–766. https://doi.org/10.1016/j.biortech.2017.06.004

Wohlert M, Benselfelt T, Wagber S, Furo I, Berglund LA, Wohlert J (2022) Cellulose and the role of hydrogen bonds: not in charge of everything. Cellulose 29(1):1–23. https://doi.org/10.1007/s10570-021-04325-4

Yan L, Ma R, Wei H, Li L, Zou B, Xu Y (2019) Ruthenium trichloride catalyzed conversion of cellulose into 5-hydroxymethylfurfural in biphasic system. Bioresour Technol 279:84–91. https://doi.org/10.1016/j.biortech.2019.01.120

Yang L, Li G, Yang F, Zhang SM, Fan HX, Lv XN (2011) Direct conversion of cellulose to 1-(furan-2-yl)-2-hydroxyethanone in zinc chloride solution under microwave irradiation. Carbohyd Res 346:2304–2307. https://doi.org/10.1016/j.carres.2011.07.005

Yoo CG, Li N, Swannell M, Pan X (2017a) Isomerization of glucose to fructose catalyzed by lithium bromide in water. Green Chem 19:4402–4411. https://doi.org/10.1039/C7GC02145C

Yoo CG, Zhang S, Pan X (2017b) Effective conversion of biomass into bromomethylfurfural, furfural, and depolymerized lignin in lithium bromide molten salt hydrate of a biphasic system. RSC Adv 7:300–308. https://doi.org/10.1039/C6RA25025D

Yu PR, Hung WC, Wan HP (2018) LiCl/HCl ionic solution for efficient conversion of lignocellulose into glucose under mild conditions. J Taiwan Inst Chem Eng 93:193–200. https://doi.org/10.1016/j.jtice.2018.07.002